

- [20] S. T. Dubas, T. R. Farhat, J. B. Schlenoff, *J. Am. Chem. Soc.* **2001**, *123*, 5368.
- [21] C. Jiang, S. Markutsya, V. V. Tsukruk, *Langmuir*, in press.
- [22] J. W. Beams, in *Structure and Properties of Thin Solid Films* (Eds: C. A. Neugebauer, J. B. Newkirk, D. A. Vermilyea), John Wiley, New York **1959**, p. 183.
- [23] J. J. Vlasak, W. D. Nix, *J. Mater. Res.* **1992**, *7*, 3242.
- [24] K. C. Grabar, R. G. Freeman, M. B. Hommer, M. J. Natan, *Anal. Chem.* **1995**, *67*, 735.
- [25] C. Jiang, S. Markutsya, V. V. Tsukruk, *Polym. Mater. Sci. Eng.* **2003**, *89*, 346.
- [26] V. V. Tsukruk, V. N. Bliznyuk, *Langmuir* **1998**, *14*, 446.
- [27] a) V. V. Tsukruk, *Rubber Chem. Technol.* **1997**, *70*, 430. b) V. V. Tsukruk, D. H. Reneker, *Polymer* **1995**, *36*, 1791.

Highly Efficient Single-Layer Polymer Electrophosphorescent Devices**

By Xiaohui Yang, Dieter Neher,* Dirk Hertel, and Thomas K. Däubler

Intense research is currently directed towards polymer light-emitting diodes (PLEDs) because of their potential for application in flat-panel displays.^[1,2] Based on their compatibility with solution processing, the exploration of their suitability for organic electronic devices has primarily been motivated by the need for low-cost production over large areas by utilizing spin-coating, ink-jet printing, or screen-printing technologies. According to simple statistics, the process of charge injection and recombination in PLEDs generates singlet excitons with a quantum efficiency of only 25 %, setting an upper limit to the efficiency of PLEDs based on fluorescent polymers. Even though the singlet–triplet ratio in PLEDs is still a topic of debate,^[3–6] it is expected that the radiative decay of both singlet and triplet states would substantially increase the efficiency of PLEDs. Phosphorescent dyes have been used to overcome the efficiency limit imposed by the unavoidable formation of triplet excitons, and highly efficient phosphorescent light-emitting diodes based on low molecular weight materials have been demonstrated.^[7–9] These high-efficiency devices typically consist of several layers including a hole-transporting layer, an emission layer doped with the phosphorescent dye, an exciton-/hole-blocking

layer and an electron-injecting layer. In fact, a multilayer LED utilizing *fac*-tris(2-phenylpyridine)iridium ($\text{Ir}(\text{ppy})_3$) as the emitting species exhibited a very high external quantum efficiency (EQE) of 19.2 % and a power conversion efficiency (PCE) of 72 lm W^{-1} at 65 cd m^{-2} .^[9]

Polymer phosphorescent light-emitting diodes (PPLEDs) usually utilize a phosphorescent dye doped into a charge-transporting polymer matrix.^[10–17] One of the criteria for the selection of the polymer matrix is that the energy of the lowest lying triplet state (T_1) of the host is larger or at least comparable to that of the phosphorescent guest. In case of $\text{Ir}(\text{ppy})_3$ with a triplet energy of about 2.4 eV, mostly non-conjugated polymers, such as poly(*N*-vinyl-carbazole) (PVK), have been used.^[11–16] In order to optimize the balance of charge-carrier injection and transport and to confine the emissive triplet excitons within the emission layer, the structure of PPLEDs generally resembles that of low molecular weight material multilayer devices.^[11–15] Yang and Tsutsui were the first to publish an efficient multilayer PPLED with a PVK: $\text{Ir}(\text{ppy})_3$ emission layer and an evaporated low molecular weight electron-transporting layer.^[11] These devices exhibited an external quantum efficiency of up to 7.5 %. A luminance of 100 cd m^{-2} was reached at about 14 V and the power conversion efficiency was 5.8 lm W^{-1} under these conditions. Lamansky et al.^[14] achieved EQEs of 3.4 % in single-layer structures by adding the low molecular weight electron-transporting molecule 2-(4-biphenyl)-5-(4-*tert*-butylphenyl)-1,3,4-oxadiazole (PBD) to the PVK host to facilitate electron transport. Vaeth and Tang^[15] reported an EQE of 8.5 % and a PCE of 9.9 lm W^{-1} at a current density of 0.5 mA cm^{-2} in a three-layer device comprising a PVK:PBD: $\text{Ir}(\text{ppy})_3$ emission layer, exciton- and hole-blocking layers, and an electron injection layer. However, combining low molecular weight materials and polymers in heterostructures compromises the unique merit of PLEDs, i.e., processing only from solutions. Gong et al.^[16] were the first to publish a high-efficiency single-layer PPLED, utilizing a chemically modified Ir-dye, tris[9,9-dihexyl-2-(pyridinyl-2')fluorene]iridium ($\text{Ir}(\text{DPF})_3$), doped into a PVK(60 wt.-%):PBD(40 wt.-%) matrix. Under optimized conditions, these single-layer devices exhibited an EQE of 10 % and a PCE of 3 lm W^{-1} . The rather low PCE was mainly due to the large operation voltage, which has been attributed to severe charge trapping on the emitter. In fact, for the optimum $\text{Ir}(\text{DPF})_3$ concentration of 1 wt.-%, a voltage of more than 20 V was needed to drive the device at a brightness of 1000 cd m^{-2} . Even though the formation of the guest triplet excited state via carrier trapping and subsequent direct carrier recombination on the guest molecule is an elegant way to achieve good color purity and high efficiency,^[10,13–16] it is often accompanied by a high operating voltage due to the build-up of a space-charge field.

In this communication, we report highly efficient single-layer PPLEDs based on a commercially available methyl-substituted iridium complex, $\text{Ir}(\text{mppy})_3$ (see inset of Fig. 4a) doped into a PVK:PBD matrix. Devices with alkyl-substituted 2-phenylpyridine (such as in $\text{Ir}(\text{bu-ppy})_3$ bearing butyl substit-

[*] Prof. D. Neher, Dr. X. Yang
Institute of Physics, University of Potsdam
Am Neuen Palais 10, D-14469 Potsdam (Germany)
E-mail: neher@rz.uni-potsdam.de
Dr. D. Hertel, Dr. T. K. Däubler
Schott Spezialglas GmbH
Hattenbergstraße 10, D-55122 Mainz (Germany)

[**] We acknowledge Frank Jaiser and Thomas Kietzke (University of Potsdam), Dr. Klaus Bonrad and Dr. Marten Walther (Schott Spezialglas GmbH) for technical support and fruitful discussions. This work was funded by the German Ministry of Science and Education. Further, financial support by the Fond der Chemischen Industrie is acknowledged.

uents) were shown to possess a significantly larger efficiency compared to similar devices utilizing Ir(ppy)₃. This improvement was attributed to a better compatibility of the alkyl-substituted Ir-complex with the host, leading to a more homogeneous distribution of the emitting molecules.^[17] We show that proper annealing before the deposition of the cathode and selection of an efficient electron-injecting cathode lead to highly efficient devices and low driving voltages. Further, the effect of the layer composition and especially of the concentration of the electron-transporting PBD in the blend is examined. We conclude that the build-up of space-charge due to trapping of holes on the Ir-complex is largely inhibited by supplying a sufficiently large number of electrons via efficient injection and transport.

Comparing the highest occupied molecular orbital (HOMO) energy of the chemically related Ir(ppy)₃ and PVK at -5.4 eV^[18] and -5.8 eV,^[13] respectively, it is evident that the guest will constitute a hole trap with a depth of ca. 0.4 eV. In contrast, the lowest unoccupied molecular orbital (LUMO) of Ir(ppy)₃ at -2.4 eV^[18] is only slightly lower than that of PVK (-2.2 eV)^[13] and comparable to that of PBD (-2.4 eV)^[19a] (please note that a PBD LUMO position of -2.4 V is commonly used in the literature, but a slightly larger electron affinity of 2.6 eV has also been published).^[19b] Evidence for carrier trapping in our Ir(mppy)₃ based devices with an as-prepared emitting layer and a Ca cathode comes from the comparison of current-voltage (*I-V*) characteristics for different Ir(mppy)₃ concentrations. As shown in Figure 1, the current-voltage characteristics shift to higher voltages with increasing concentration of Ir(mppy)₃, consistent with earlier reports that iridium complexes constitute hole traps in a PVK host.^[13-16] The largest increase in voltage is observed when going from 1 wt.-% to 2 wt.-%, while further increasing the Ir(mppy)₃ concentration to 8 wt.-% causes a much smaller

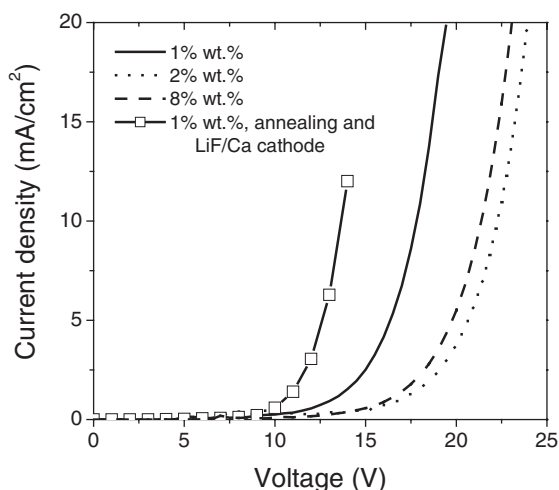


Figure 1. Current-voltage characteristics of devices with different Ir(mppy)₃ concentrations (not annealed, Ca cathode). Also shown is the *I-V* curve of a device with an annealed emission layer and a 1 nm thick LiF interfacial layer. The layer thickness was 100 nm in each case.

shift of the *I-V* curves. This observation is similar to what has been reported by Noh et al. for a PVK:Ir(ppy)₃ blend (in this case, the current at a Ir(ppy)₃ concentration of 8 wt.-% was even larger than at 1 wt.-%).^[20] Most likely, the direct hopping of holes between Ir dyes becomes possible at higher concentrations, without the need for detrapping to the PVK host. Similar conclusions have been drawn earlier from time-of-flight studies on PVK doped with the hole-transporting molecule *N,N'*-diphenyl-*N,N'*-(bis(3-methylphenyl)-[1,1-biphenyl]-4,4'-diamine (TPD)).^[21] In addition, hole injection from the poly(3,4-ethylenedioxy thiophene):poly(styrene sulfonate) (PEDOT:PSS) anode might be facilitated at higher dye concentrations via direct charge transfer to the HOMO of Ir(mppy)₃.

The driving voltage could be reduced by annealing the sample at 80 °C before the deposition of the cathode (data shown in Table 1). This suggests that the build-up of a space-charge field is less severe in the annealed devices. Concurrently, the efficiency of the devices was significantly improved. The lumi-

Table 1. Performance of phosphorescent polymer light-emitting diodes with either an as-prepared or an annealed (30 min at 80 °C) emission layer and with different cathode configurations.

Device	Current density [mA cm ⁻²]	Voltage [V]	Brightness [cd m ⁻²]	Efficiency [cd A ⁻¹]
Without annealing, Ca cathode [a]	2.8	9.9	504	17.7
With annealing, Ca cathode [a]	2.8	8.9	602	21.1
Without annealing, LiF/Ca cathode [a]	11.4	10.6	2210	19.4
With annealing, LiF/Ca cathode [a]	2.8	7.9	655	23.0
Without annealing, LiF/Ca cathode [b]	11.4	9.7	2230	19.6
Without annealing, LiF/Ca cathode [b]	15	10.1	171	1.1
With annealing, LiF/Ca cathode [b]	15	9.2	238	1.6

[a] PEDOT (30 nm) / PVK(70):PBD(29):Ir(mppy)₃(1) (70 nm). [b] PEDOT (30 nm) / PVK(69):PBD(28):btp₂Ir(acac)(3) (70 nm).

nance efficiency of the devices that have undergone annealing was about 20 % higher than that of devices without thermal treatment, and at the same time the driving voltage for a certain current density decreased by about 12 %. In total, annealing led to a ca. 37 % improvement of the PCE, resulting in ca. 7.5 lm W⁻¹ at a brightness of 600 cd m⁻². Since annealing the samples at 60 °C for 0.5 h did essentially not change the performances of the devices, we presume that the improvement of the device performances upon annealing is most likely not related to uncompleted removal of residual solvent in the as-prepared layers. At the moment we can only speculate about the reason for this improvement. Nguyen et al.^[22] observed a ca. 50 % higher EQE for devices based on annealed poly(2-methoxy-5-(2'-ethylhexyloxy)-1,4-phenylenevinylene) (MEH-PPV) layers. It was suggested that electron injection was improved by better interfacial contact due to the smooth surface

of the annealed MEH-PPV film. A significant improvement in device efficiency has also been observed when annealing a multicomponent polymer emission layer prior to the deposition of the cathode. In this case, atomic force microscope (AFM) studies revealed significant morphological changes, including the formation of phase-separated structures.^[23] Detailed AFM studies need to be performed in future work to identify the main mechanism leading to the improvement in device performance reported here.

The operating voltage could be further decreased by 9–12 % by adding a LiF layer between the polymer and the Ca cathode. A ca. 10 % enhancement of the luminance efficiency was observed in the low current density regime. It is well established that introducing a thin metal fluoride layer between an organic layer and low work function metals, such as Ca or Yb, improves the performance of organic light-emitting devices.^[24,25] Electro-absorption experiments demonstrated that adding a thin LiF layer between a polymeric emitting layer and Ca decreases the barrier height for electron injection by ca. 0.28 eV.^[24] In our device, there is a significant energy barrier for electron injection due to the difference between the electron affinity of PBD (ca. 2.4 eV) and the work function of Ca (2.9 eV). It can thus be concluded that introducing a thin LiF layer improves electron injection into the PVK:PBD host of our devices. In combination with annealing, adding a LiF interfacial layer reduces the driving voltage by several volts, as shown by the *I*–*V* characteristics in Figure 1 and the data listed in Table 1. As a result, these devices exhibit large PCE efficiencies of 9 lm W⁻¹ at ca. 650 cd m⁻² and 6.3 lm W⁻¹ at 2230 cd m⁻². Note that the annealing treatment was found to be even more beneficial for the performances of devices with the red phosphorescent dye, iridium bis(2-(2'-benzo[4,5-a]thienyl)pyridinato-*N,C*^{3'}) (btp₂Ir(acac)).^[26] In this case, we even observed a 40 % and 54 % improvement of the luminance efficiency and PCE, respectively.

The devices reported so far were based on a blend of the hole-transporting PVK matrix and the electron-transporting PBD at a weight ratio of ca. 70:30. To further understand how charge transport and charge-carrier trapping affect the device properties, we studied devices with different concentrations of the electron-transporting moiety PBD and of the hole-trapping Ir(mppy)₃ complex. As a third crucial parameter, the layer thickness was varied over a wide range. In order to minimize the number of devices in this optimization step, a statistical approach was utilized.^[27,28] Details about this approach will be published elsewhere. In short, 13 different devices with PBD concentrations *c*_{PBD} ranging between ca. 10 and 35 wt.-%, Ir(mppy)₃ concentrations *c*_{Ir} between ca. 0.3 and 7 wt.-% and PVK layer thicknesses *d*_{PVK} between 50 and 110 nm were examined. In all cases, the emissive layers were annealed and an interfacial LiF layer

was added before deposition of the Ca/Al cathode. Current–brightness–voltage characteristics of the different devices were recorded and, in the analysis of the data, various device properties, such as the luminance efficiency and the driving voltage, were compared at certain current densities. Then, each of these device properties (denoted here as *P*(*c*_{PBD}, *c*_{Ir}, *d*_{PVK})) was separately fitted to a second-order polynomial function of the variables *c*_{PBD}, *c*_{Ir}, and *d*_{PVK}:

$$P(c_{\text{PBD}}, c_{\text{Ir}}, d_{\text{PVK}}) = A_1 c_{\text{PBD}} + A_2 c_{\text{PBD}}^2 + B_1 c_{\text{Ir}} + B_2 c_{\text{Ir}}^2 + C_1 d_{\text{PVK}} + C_2 d_{\text{PVK}}^2 + D c_{\text{PBD}} c_{\text{Ir}} + E c_{\text{PBD}} d_{\text{PVK}} + F c_{\text{Ir}} d_{\text{PVK}} \quad (1)$$

This results in nine fitting coefficients *A*–*F* for each device property. However, for the devices studied here, only few of these coefficients had values with statistical significance. Most importantly, both the efficiency and the driving field depended clearly on the concentration of PBD, while they were only weakly affected by the concentration of the Ir dye. As an example, Figure 2a shows the resulting multiparameter fitting function to the electric field at a constant current density

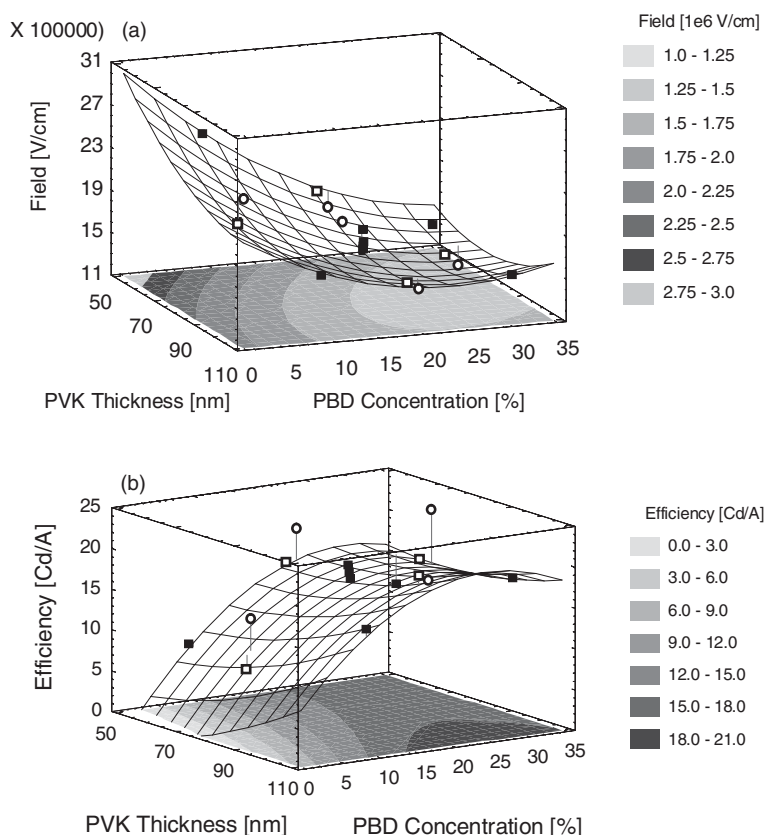


Figure 2. Results of the statistical analysis of the dependence of the electric field (a) and the luminance efficiency (b) on the PBD concentration, the PVK layer thickness, and the Ir(mppy)₃ concentration. Symbols show the experimental data measured at a constant current density of 5 mA cm⁻² for devices with Ir(mppy)₃ concentrations of 0.3–0.5 wt.-% (open circles), 2.5–4 wt.-% (solid squares), and 5–7 wt.-% (open squares). The response surface and contour plots present the corresponding multiparameter functions according to Equation 1, obtained from the best fit to the experimental data, plotted for a fixed Ir(mppy)₃ concentration *c*_{Ir} of 3.5 wt.-%.

of 5 mA cm^{-2} , plotted as a function of c_{PBD} and d_{PVK} for a fixed value of $c_{\text{Ir}} = 3.5 \text{ wt.-%}$ (similar plots were obtained with different values of c_{Ir} in the investigated range from 0.3 to 7 wt.-%). Also shown are the measured data points (symbols). Even though these data were measured for devices with very different $\text{Ir}(\text{mppy})_3$ concentration, most data points lie close to the response surface plot of the multi-parameter fitting function, calculated for a constant $\text{Ir}(\text{mppy})_3$ concentration. This illustrates that varying the $\text{Ir}(\text{mppy})_3$ concentration does not significantly influence the driving field. Furthermore, at high PBD concentrations, there is no dependence of the driving field on the layer thickness. Apparently, the device current is mainly injection-limited under these conditions. We, therefore, presume that the space-charge formed by hole trapping on the $\text{Ir}(\text{mppy})_3$ can be effectively neutralized by efficient injection and transport of electrons in our devices.

The corresponding response-surface plot of the fit to the luminance efficiency is shown in Figure 2b. Again, the concentration of the electron-transporting moiety in the layer apparently is a major parameter controlling the device performance. Also, the rather small scatter of the data around the fitting function (calculated for a constant value of c_{Ir}) suggests, that the $\text{Ir}(\text{mppy})_3$ concentration has only a weak influence on the device efficiency. However, there are few data points situated well above the fit. All these points belong to devices with an $\text{Ir}(\text{mppy})_3$ concentration smaller than 0.5 wt.-%. Obviously, a small $\text{Ir}(\text{mppy})_3$ concentration is beneficial to obtain high efficiencies, similar to what has been reported by Gong et al. in their recent papers.^[16,29] At the moment, we can only speculate about the reason for this effect. Interestingly, the photoluminescence (PL) spectra measured for different $\text{Ir}(\text{mppy})_3$ concentrations with direct excitation of the Ir complex at 400 nm (Fig. 3a) exhibit a well-resolved shift of the PL maximum with increasing concentration. Further, the same spectra normalized to the absolute $\text{Ir}(\text{mppy})_3$ concentration (Fig. 3b) show a lower intensity for higher concentrations. These observations are indicative of intermolecular interaction between the Ir complexes, opening new channels for non-radiative triplet decay.

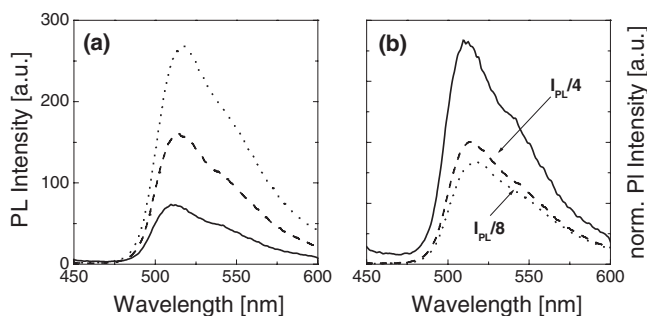


Figure 3. a) Photoluminescence spectra of blend layers with different concentrations of $\text{Ir}(\text{mppy})_3$ doped into a PVK(70):PBD(30) matrix, measured upon direct excitation of the Ir-complex at 400 nm. Shown are spectra for an absolute concentration of $\text{Ir}(\text{mppy})_3$ of 1 wt.-% (solid line), 4 wt.-% (dashed line), and 8 wt.-% (dotted line). b) Emission spectra normalized to the absolute concentration of $\text{Ir}(\text{mppy})_3$.

We would like to point out that the comparison of the PL spectra of the blends, excited at the absorption peak of PVK, and the electroluminescence (EL) spectra (not shown here) provides strong evidence that the main pathway for exciting the triplet state of the Ir complex in EL is carrier trapping and recombination on the guest. In fact, while a concentration of ca. 7–8 wt.-% of $\text{Ir}(\text{mppy})_3$ was necessary to completely quench the PVK emission in PL, the EL spectra did not exhibit any emission from the host even at concentrations as low as 0.5 wt.-%. On the other hand, the data in Figure 2b combined with the normalized PL spectra in Figure 3b suggest that the total number of guest triplet excitons formed in the emission layer per time and unit area at a given current density is rather independent of the concentration of the hole-trapping Ir complex. This indicates that the capture of charges by the individual guest molecules is not the main step limiting the kinetics of triplet formation on the phosphorescent Ir complexes.

We were able to improve the device efficiency further by increasing the PEDOT:PSS layer thickness from 30 nm to 70 nm. The reason for this effect is not known yet. A further reduction in driving voltage was achieved by replacing the LiF/Ca cathode with a CsF/Al cathode, which was shown earlier to improve electron injection.^[30,31] Figure 4a shows the current–brightness–voltage characteristics of such a device with a PBD concentration of 30 wt.-% and an $\text{Ir}(\text{mppy})_3$ concentration of 1 wt.-%. Figure 4b displays the dependence of the luminance efficiency and the PCE on the current density of the devices. The turn-on voltage (0.1 cd m^{-2}) of the device was 3.5 V. The maximum luminance efficiency was 27 cd A^{-1} at a current density of 2.3 mA cm^{-2} and a brightness of 612 cd m^{-2} , corresponding to an EQE of 7.6 %. The luminance efficiency of our devices is comparable to the best data achieved in the devices utilizing an Ir complex blended into a polymer matrix.^[11–17] Note that an even higher luminance efficiency (36 cd A^{-1}) and a higher external quantum efficiency (10 %) (measured with an integrating sphere) were reported using $\text{Ir}(\text{DPF})_3$ in a similar single-layer device structure.^[16] But in this case, the operating voltage was remarkably higher, leading to a rather low PCE of ca. 3 lm W^{-1} . In our devices, the peak PCE was 14.1 lm W^{-1} at a driving voltage of 5.5 V, a current density of 0.7 mA cm^{-2} , and a brightness of 170 cd m^{-2} . This is well above most values reported for single- and multilayer PPLEDs. Even though the luminance efficiency and power efficiency of our devices decreased gradually with increasing current density, the luminance efficiency was still 23.4 cd A^{-1} at a current density of 20 mA cm^{-2} , an operating voltage of 8.9 V and a brightness of 4680 cd m^{-2} , corresponding to an EQE of 6.6 % and a PCE of 8.3 lm W^{-1} . This is well above the so-called upper limit of EQE (5 %) of most devices utilizing fluorescent polymers reported so far, demonstrating the benefit of triplet harvesting. We finally would like to note that a single layer device with comparable efficiencies (PCE of 12.8 lm W^{-1} at a luminance of 500 cd m^{-2}), based on a spin-coated layer of a first generation $\text{Ir}(\text{ppy})_3$ -cored dendrimer, was reported recently.^[32] However, the preparation of

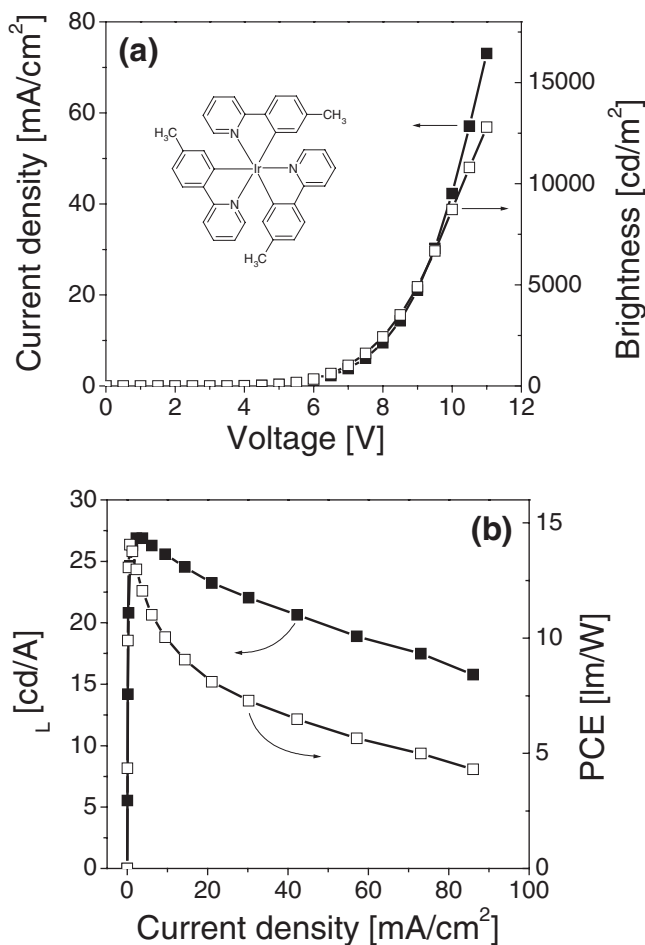


Figure 4. a) Current–brightness–voltage characteristics of a device with a 70 nm thick PEDOT:PSS layer and a CsF(1 nm)/Al cathode. Also shown are the corresponding curves for the luminance efficiency and the PCE as a function of the current density (b). The absolute Ir(mppy)₃ concentration in the PVK(70):PBD(30) host was 0.7 wt.-%.

dendrimers requires more elaborated chemistry, and therefore this approach might turn out to be less applicable to large-scale production.

In conclusion, highly efficient single-layer PPLEDs based on a commercially available Ir complex have been realized by appropriate thermal treatment of the polymer layer, utilization of efficient bilayer cathodes, and proper adjustment of the layer composition. In fact, these devices exhibited essentially no dependence of the driving field on the concentration of the Ir complex, suggesting that the build-up of space-charge in the layer is insignificant. We presume that holes trapped on the emitter are effectively neutralized via efficient injection, transport, and recombination of electrons in these optimized devices. As a consequence, our devices exhibit low driving voltages and a power conversion efficiency of up to 14.1 lm W⁻¹. This is comparable to the highest values reported for polymer-based phosphorescent devices so far.

Experimental

Ir(mppy)₃ was obtained from American Dye Sources and used as received. Poly(3,4-ethylenedioxy thiophene) doped with poly(styrene sulfonate) (PEDOT:PSS) (Baytron P purchased from H.C. Starck) was spin-coated onto pre-cleaned and O₂-plasma treated indium tin oxide (ITO) substrates, yielding layers with a thickness of ca. 30 nm. The PEDOT:PSS layers were baked at 100 °C for 0.5 h to remove residual water. A blend of PVK, PBD, and Ir(mppy)₃ in chlorobenzene solution was spin-coated on top of the PEDOT:PSS film. In some cases, the sample was then annealed at 80 °C for 30 min. The devices were completed by thermal deposition of cathode metals. In some devices, an ultrathin LiF or CsF interfacial layer with a nominal thickness of 1 nm was incorporated between the polymer layer and the cathode metals (Ca or Al). Current–voltage characteristics were measured with a Keithley 2400 source measure unit. The brightness of the devices was recorded with a Minolta CS-100A camera. EL spectra of the devices were measured using a charge-coupled device (CCD) fiber spectrometer (Ocean Optics). With the exception of the deposition of the PEDOT:PSS layer, all processes were carried out in dry nitrogen atmosphere.

Received: July 1, 2003
Final version: October 10, 2003

- [1] R. H. Friend, R. W. Gymer, A. B. Holmes, J. H. Burroughes, R. N. Marks, C. Taliani, D. D. C. Bradley, D. A. Dos Santos, J.-L. Bredas, M. Logdlund, W. R. Salaneck, *Nature* **1999**, *397*, 121.
- [2] A. J. Heeger, *Angew. Chem. Int. Ed.* **2001**, *40*, 2591.
- [3] Y. Cao, I. D. Parker, G. Yu, C. Zhang, A. J. Heeger, *Nature* **1999**, *397*, 414.
- [4] M. Wohlgenannt, K. Tandon, S. Mazumdar, S. Ramasesha, Z. V. Vardeny, *Nature* **2001**, *409*, 494.
- [5] J. S. Wilson, A. S. Dhoot, A. J. A. B. Seeley, M. S. Khan, A. Köhler, R. H. Friend, *Nature* **2001**, *413*, 828.
- [6] A. S. Dhoot, N. C. Greenham, *Adv. Mater.* **2002**, *14*, 1834.
- [7] M. A. Baldo, D. F. O'Brien, Y. You, A. Shoustikov, S. Sibley, M. E. Thompson, S. R. Forrest, *Nature* **1998**, *395*, 151.
- [8] M. A. Baldo, S. Lamansky, P. E. Burrows, M. E. Thompson, S. R. Forrest, *Appl. Phys. Lett.* **1999**, *75*, 4.
- [9] M. Ikai, S. Tokito, Y. Sakamoto, T. Suzuki, Y. Taga, *Appl. Phys. Lett.* **2001**, *79*, 156.
- [10] P. A. Lane, L. C. Palilis, D. F. O'Brien, C. Giebeler, A. J. Cadby, D. G. Lidzey, A. J. Campbell, W. Blau, D. D. C. Bradley, *Phys. Rev. B* **2002**, *63*, 235206.
- [11] M.-J. Yang, T. Tsutsui, *Jpn. J. Appl. Phys.* **2000**, *39*, 828.
- [12] C.-L. Lee, K. B. Lee, J.-J. Kim, *Appl. Phys. Lett.* **2000**, *77*, 2280.
- [13] Y. Kawamura, S. Yanagida, S. R. Forrest, *J. Appl. Phys.* **2002**, *92*, 87.
- [14] S. Lamansky, P. I. Djurovich, F. A. Razzaq, S. Garon, D. L. Murphy, M. E. Thompson, *J. Appl. Phys.* **2002**, *92*, 1570.
- [15] K. M. Vaeth, C. W. Tang, *J. Appl. Phys.* **2002**, *92*, 3447.
- [16] X. Gong, M. R. Robinson, J. C. Ostrowski, D. Moses, G. C. Bazan, A. J. Heeger, *Adv. Mater.* **2002**, *14*, 581.
- [17] W. G. Zhu, Y. Q. Mo, M. Yuan, W. Yang, Y. Cao, *Appl. Phys. Lett.* **2002**, *80*, 2045.
- [18] D. Kolosov, V. Adamovich, P. Djurovich, M. E. Thompson, C. Adachi, *J. Am. Chem. Soc.* **2002**, *124*, 9945.
- [19] a) S. Janietz, A. Wedel, *Adv. Mater.* **1997**, *9*, 403. b) C. H. Kim, J. Shinar, *Appl. Phys. Lett.* **2002**, *80*, 2201.
- [20] Y.-Y. Noh, C.-L. Lee, J.-J. Kim, K. Yase, *J. Chem. Phys.* **2003**, *118*, 853.
- [21] D. M. Pai, J. F. Yanus, M. Stolka, *J. Phys. Chem.* **1984**, *88*, 4714.
- [22] T.-Q. Nguyen, R. C. Kwong, M. E. Thompson, B. J. Schwartz, *Appl. Phys. Lett.* **2000**, *76*, 2454.

- [23] H. Hänsel, D. C. Müller, M. Gross, K. Meerholz, G. Krausch, *Macromolecules* **2003**, *36*, 4932.
- [24] T. M. Brown, R. H. Friend, I. S. Millard, D. J. Lacey, J. Burroughes, F. Cacialli, *Appl. Phys. Lett.* **2001**, *79*, 174.
- [25] M. Y. Chan, S. L. Lai, M. K. Fung, S. W. Tong, C. S. Lee, S. T. Lee, *Appl. Phys. Lett.* **2003**, *82*, 1784.
- [26] S. Lamansky, P. Djurovich, D. Murphy, F. A. Razzaq, H.-E. Lee, C. Adachi, P. E. Burrows, S. Forrest, M. E. Thompson, *J. Am. Chem. Soc.* **2001**, *123*, 4304.
- [27] G. E. P. Box, W. G. Hunter, J. S. Hunter, *Statistics for Experimenters*, John Wiley, New York **1978**.
- [28] H. Toutenburg, *Versuchsplanung und Modellwahl*, Physica-Verlag, Heidelberg **1994**.
- [29] X. Gong, J. C. Ostrowski, D. Moses, G. C. Bazan, A. J. Heeger, *Adv. Funct. Mater.* **2003**, *13*, 439.
- [30] G. E. Jabbour, J. F. Wang, B. Kippelen, N. Peyghambarian, *Jpn. J. Appl. Phys.* **1999**, *38*, 1553.
- [31] X. Yang, Y. Mo, W. Yang, Y. Cao, *Appl. Phys. Lett.* **2001**, *79*, 563.
- [32] T. D. Anthopoulos, J. P. J. Markham, E. B. Nambas, I. D. W. Samuel, S.-C. Lo, P. L. Burn, *Appl. Phys. Lett.* **2003**, *82*, 4824.

Use of Coaxial Gas Jackets to Stabilize Taylor Cones of Volatile Solutions and to Induce Particle-to-Fiber Transitions**

By *Gustavo Larsen,* Rubén Spretz, and Raffet Velarde-Ortiz*

Over the last few years there has been increasing interest in the use of electrohydrodynamics (EHD) to manufacture micro- and nanometer-scale architectures such as fibers, vesicles, and hollow structures. A vast array of inorganic,^[1] hybrid (organic/inorganic) materials,^[1,2] and organic polymers^[3] has been produced using EHD. Potential applications encompass a wide spectrum of fields, and include membrane technologies,^[4] reinforced materials,^[5] textiles,^[6] optical sensors,^[7] drug delivery systems,^[8] and tissue engineering.^[9]

In the usual EHD set-up a relatively small flow of liquid (in the nanoliters to microliters per minute range) is pumped through a capillary tube, initially forming a droplet-like meniscus attached to the capillary's tip. A high voltage is applied between the tip and a grounded metallic surface or "collector" electrode. As the applied voltage increases, the droplet takes a conical shape called a Taylor cone and from its apex a very fine jet of liquid is accelerated and expelled towards the collector.

The ultimate form of the collected material can be tailored by tuning the concentration of the different components, conductivity, surface tension, and chemical nature of the solution. In the case of fiber synthesis, the appearance of beaded fibers or bead-free fibers can be controlled by manipulating the viscosity, conductivity, and surface tension of the system.^[3,10,11] With regard to beaded nanofiber production, a strategy that has proven useful is to use corona discharges to partially—and locally—neutralize the electrified liquid jet.^[3]

In systems where the solvent used has a low boiling point, the droplet at the tip dries out very quickly during, or before, the formation of the Taylor cone, thereby blocking the tip and making the collection process discontinuous or even impossible to carry out.^[11–13] Several alternatives have been proposed to overcome this problem. One is the use of a compatible co-solvent to increase the boiling point of the solution. In this case some experimentation is needed to determine the suitable co-solvent to be used as well as its concentration. A less intrusive alternative is to run the process at lower temperatures or at least confine the capillary tip and the collector in a solvent saturated atmosphere.

In this work we present a versatile method that makes the process continuous and stable, thereby avoiding the need for periodic clean-up of the EHD tip. An added "bonus" of the proposed technique is that it also offers the possibility to control morphology transitions from fibers to beaded fibers or particles without changing the operating voltage or electric current. This is achieved by using a nozzle consisting of two coaxial capillary tubes. The inner tube delivers the working solution, while the outer one delivers a controlled flow of an inert gas saturated with the corresponding solvent of the solution to be subjected to EHD. If a "jacket" gas with high ionization potential is used, an additional advantage of this set-up becomes apparent: the suppression of corona discharges that might otherwise occur when processing aqueous systems with very high surface tension in an air atmosphere. In such cases, very high voltages are typically needed to form Taylor cones.^[14] This basic set-up could then be extended to multiple capillaries for the production of coatings and hollow structures.

We have successfully used this approach in our lab for several inorganic precursors (Al₂O₃, SiC,^[15] SiO₂), organic polymers (polystyrene), and biopolymers (starch acetate).^[15] For brevity two model systems are discussed here: poly(L-lactide) (PLA) and ZrO₂.

Figure 1 shows the influence of the operating variables on the ability of PLA solutions to stabilize Taylor cone structures. When a 10 wt.-% PLA solution in dichloromethane (DCM) is electrospun at a 0.8 kV cm⁻¹ with a jacketing flow of DCM-saturated N₂, a stable Taylor cone develops. This stable electrified meniscus structure is maintained until the whole 10 mL volume of the syringe attached to the digital pump is discharged (Fig. 1b). Varying the flow rate of solvent-saturated N₂ in the range of 8–80 cm³ min⁻¹ was found to have no effect on the Taylor cone structure. As expected, changes in the applied voltage affect the conditions at which the solu-

[*] Prof. G. Larsen, Dr. R. Spretz, R. Velarde-Ortiz
Department of Chemical Engineering
University of Nebraska-Lincoln
Lincoln, NE 68588-0643 (USA)
E-mail: glarsen@unlserve.unl.edu

[**] We thank the National Science Foundation for financial support under grant CTS-0129190. We are very grateful to Dr. Ignacio Gonzalez Loscertales for fruitful discussions.